S1. Theoretical calculation for the scattering length density (SLD) of a molecule. Theoretically, the SLD of a molecule is computable via its molecular structure and mass density. Thus, b_{graft} = 1.234, 1.307 and 1.342 (× 10^{10} cm^{-2}) for each AEM are estimated as listed in Table 2.[52] The exact mass density of either ETFE crystalline or amorphous chain is unknown; however, plenty of previous reports showed that the scattering intensity of the neat ETFE base films is very weak, suggesting a negligible small difference in the SLD of ETFE crystalline and amorphous domains.[14, 16, 50] Therefore, it is reasonable to use the average mass density of ETFE film of 1.7 g/cm^3 to roughly estimate the SLD of ETFE crystalline and amorphous domains to be 2.7 × 10^{10} cm^{-2} as listed in Table 2. b_w is a function of f_{D2O} given by

$$b_w = b_{D2O} f_{D2O} + b_{H2O}(1 - f_{D2O}) \quad \text{(S1)}$$

where b_{D2O} and b_{H2O} are the SLD of D_2O and H_2O being 6.34 and -0.56 (× 10^{10} cm^{-2}), respectively.[52]

S2. Hard-Sphere fluid model analysis. For the identical spheres, $P(q)$ is expressed as a functions of an average radius (R_s) and the standard deviation of R_s (σ_R) as below.

$$P(q) = v^2\{\frac{3[\sin(qR_s) - qR_s\cos(qR_s)]}{(qR_s)^3}\}^2 \quad \text{(S2)}$$

with v being the volume of the sphere as $v = (4\pi R_s^3)/3$. For spheres with a size distribution, Gaussian distribution function is applied to modify $P(q)$ as[52]

$$P(q) = \int_0^\infty v^2\left\{\frac{3}{(qr)^3}[\sin(qr) - qr\cos(qr)]\right\}^2 \times \frac{1}{(2\pi)^{1/2}\sigma_R} exp[\frac{-(r - R_s)^2}{2{\sigma_R}^2}]dr \quad \text{(S3)}$$

where σ_R is the standard deviation of R_s.

Given that Percus–Yevick approximation accounts for the inter-particle interference, $S(q)$ is expressed as a function of the volume fraction of spheres (ϕ_s) and R_s.[53-55]

$$S(q) = \frac{1}{1 + 24\phi_s(\frac{F(A)}{A})} \quad \text{(S4)}$$

where $A = 2qR_s$, ϕ_s is the volume fraction of spheres in the conducting domains, and $F(A)$ is a trigonometric function of A by

$$F(A) = \frac{\alpha}{A^2}(sinA - AcosA) + \frac{\beta}{A^3}\left(2AsinA + \left(2 - A^2\right)cosA - 2\right) + \frac{\gamma}{A^5}\left(-A^4co$$

(S5)

where

$$\alpha = \left(1 + 2\phi_s\right)^2/\left(1 - \phi_s\right)^4$$
$$\beta = -6\phi_s\left(1 + \frac{\phi_s}{2}\right)^2/(1 - \phi_s)^4$$
$$\gamma = \frac{1}{2\phi_s}\left(1 + 2\phi_s\right)^2/(1 - \phi_s)^4 \quad \text{(S6)}$$

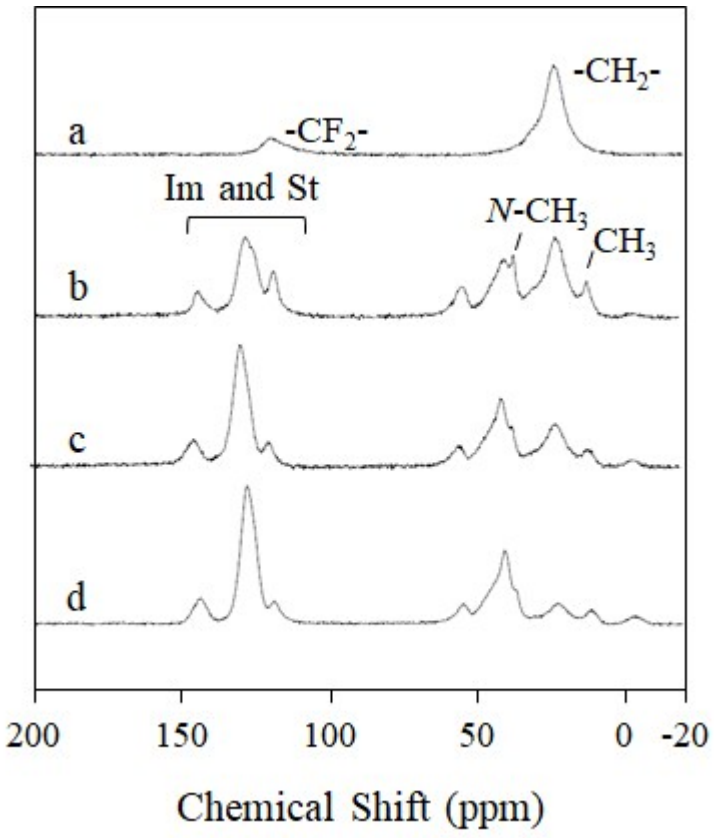

Figure S1 ^{13}C solid-state NMR spectra of (a) a ETFE base film, and (b) Im_6St_4-, (c) Im_4St_6-, (d) Im_3St_7- AEMs in the Cl^- form.

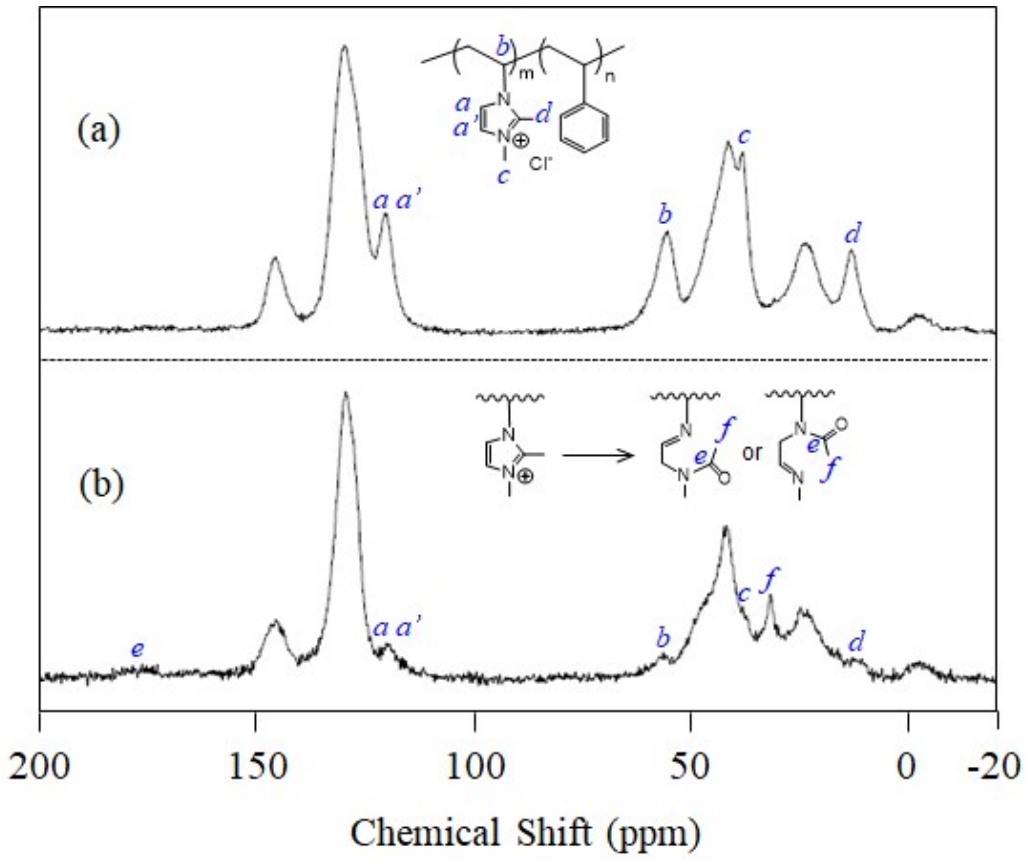

Figure S2 ^{13}C solid-state NMR spectra of Im_6St_4[ref14] in the Cl^- form (a) before, and (b) after immersion in 1 M KOH solution at 80 °C for 740 h.

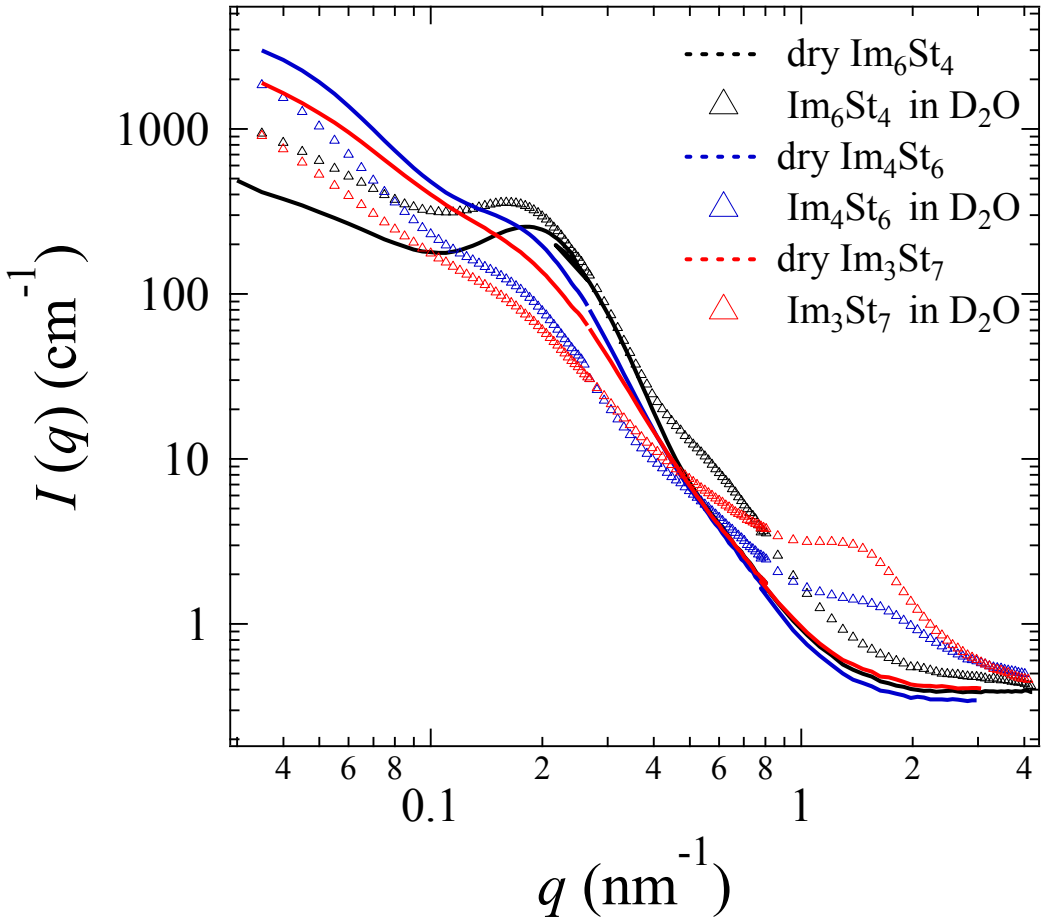

Figure S3 SANS intensity profiles of Im_6St_4-, Im_4St_6- and Im_3St_7-AEMs in the dry state and equilibrated in D_2O before incoherent scattering correction.

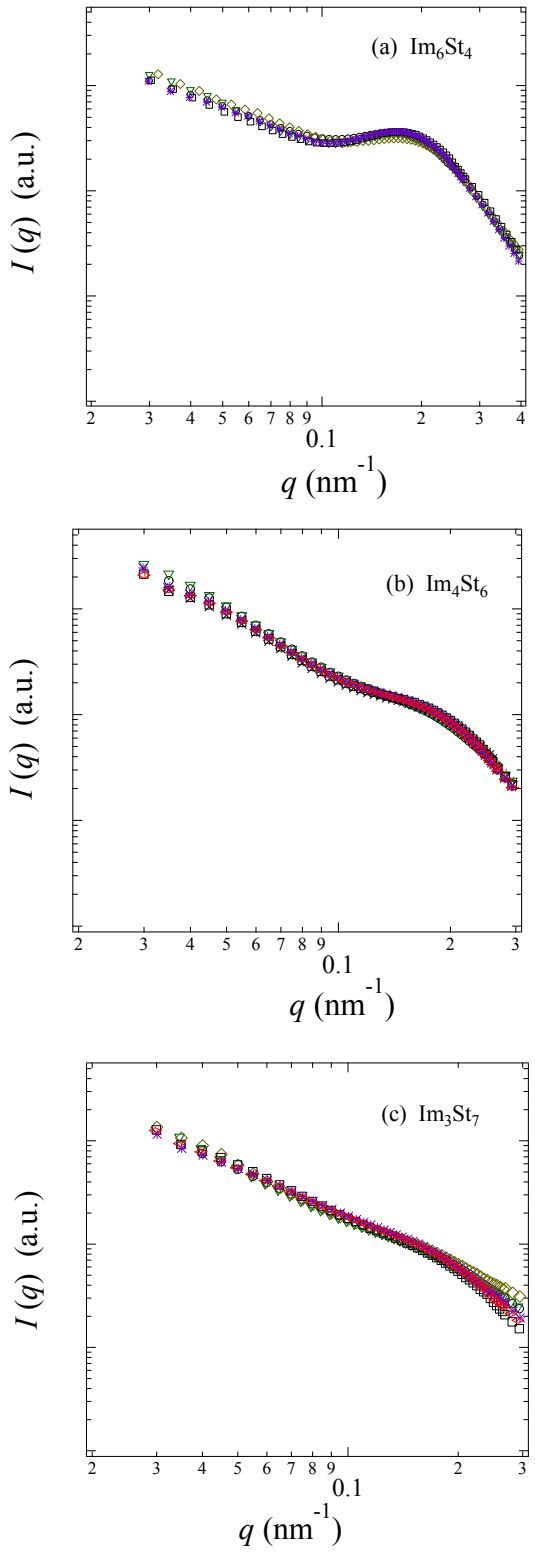

Figure S4 Normalization of I(q) profiles at around the first-order lamellar peaks in Region I for (a) Im_6St_4-, (b) Im_4St_6- and (c) Im_3St_7-AEMs, respectively.

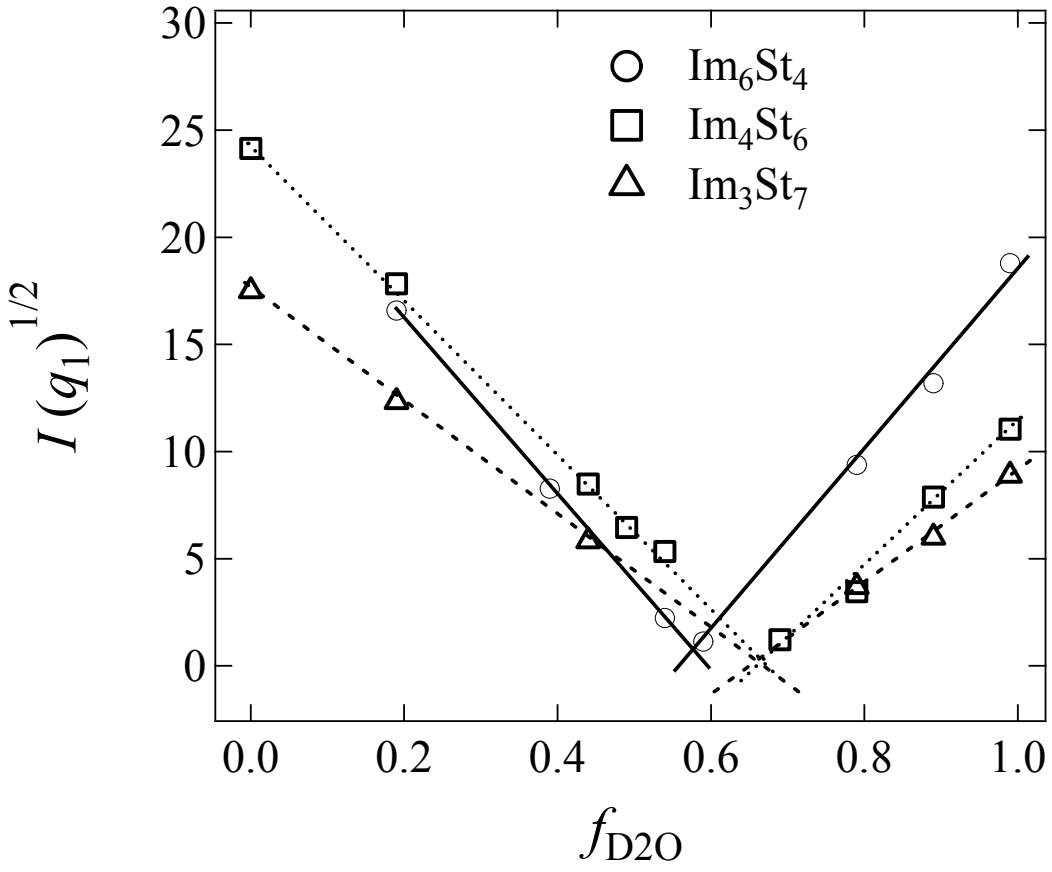

Figure S5 The volume fraction f_{D2O} dependence of $I(q_1)^{1/2}$ observed for AEMs swollen in water mixtures shown in Figure 4.

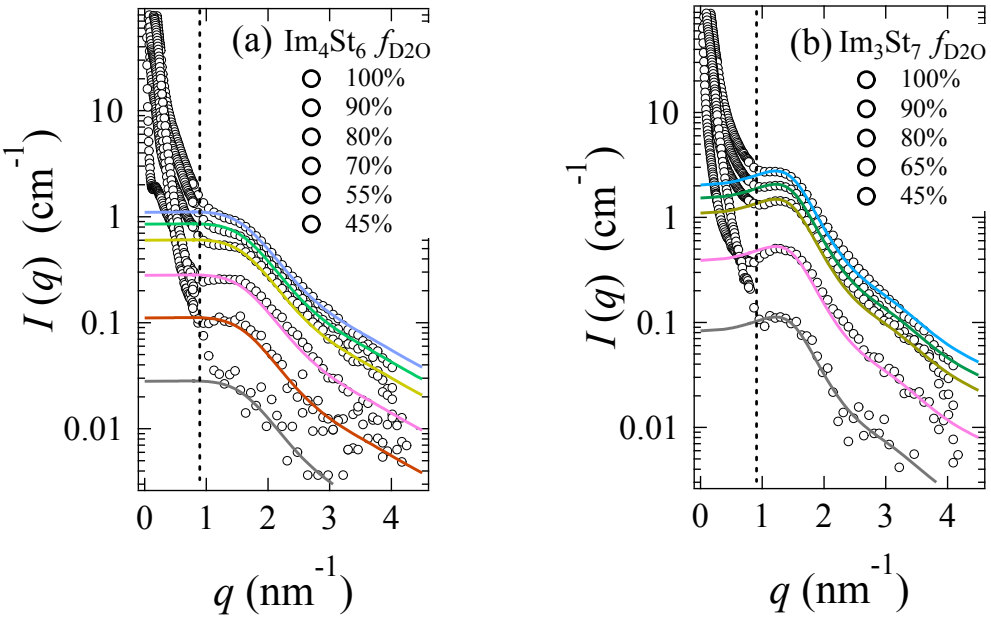

Figure S6 $I(0)_{exp}$ can be estimated by experimentally extrapolating the best-fitted lines to $q \sim 0$ for all contrasts SANS profiles (symbols) obtained from (a) Im_4St_6-AEM and (b) Im_3St_7-AEM, respectively.

Table S1 WU and SR for AEMs in OH^- form at 25 °C

AEMs in OH^- form	Im/St	GD (%)	WU (%)	SR (%)
Im_6St_4	62/38	30	46	55
Im_4St_6	42/58	53	55	71
Im_3St_7	26/74	110	79	78

Table S2 Parameters used to fit SANS profiles of Im_4St_6 and Im_3St_7 membranes equilibrated in water mixtures by eq. (11)

f_{D2O}	Im_4St_6				Im_3St_7			
(%)	ϕ_s	R_s (nm)	σ_R/R_s	K	ϕ_s	R_s (nm)	σ_R/R_s	K
0				0.63				2.1
20				0.06				0.51
45				0.06				0.38
50				0.16				-
55	0.12	1.6	0.28	0.55	0.195	2.0	0.26	-
65				-				1.79
70				0.59				-
80				1.16				5.06
90				1.58				7.03
100				2.1				9.4